Modeling of Charge Transfer Inefficiency in a CCD With High-Speed Column Parallel Readout

André Sopczak, *Member, IEEE*, Salim Aoulmit, Khaled Bekhouche, Chris Bowdery, Craig Buttar, Chris Damerell, Dahmane Djendaoui, Lakhdar Dehimi, Tim Greenshaw, Michal Koziel, Dzmitry Maneuski, Andrei Nomerotski, Konstantin Stefanov, Tuomo Tikkanen, Tim Woolliscroft, and Steve Worm

***Abstract*—Charge Coupled Devices (CCDs) have been successfully used in several high energy physics experiments over the past two decades. Their high spatial resolution and thin sensitive layers make them an excellent tool for studying short-lived particles. The Linear Collider Flavour Identification (LCFI) collaboration is developing Column-Parallel CCDs (CPCCDs) for the vertex detector of a future Linear Collider. The CPCCDs can be read out many times faster than standard CCDs, significantly increasing their operating speed. An Analytic Model has been developed for the determination of the charge transfer inefficiency (CTI) of a CPCCD. The CTI values determined with the Analytic Model agree largely with those from a full TCAD simulation. The Analytic Model allows efficient study of the variation of the CTI on parameters like readout frequency, operating temperature and occupancy.**

***Index Terms*—CCD detectors, charge coupled devices, charge transfer efficiency, Linear Collider vertex detectors, position sensitive detectors, radiation damage.**

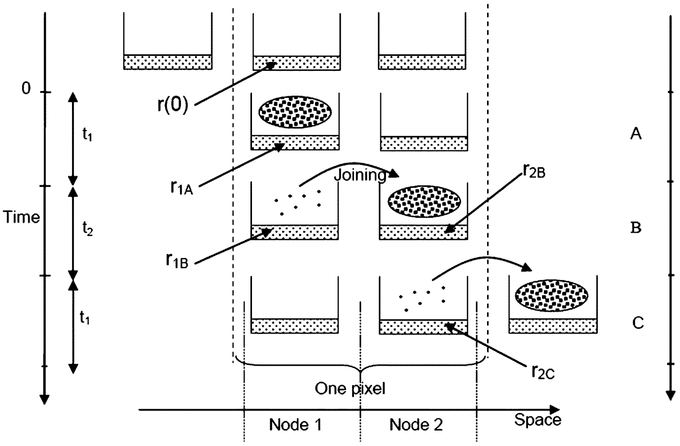

Fig. 1. Diagram of consecutive transfer of charge in a two-phase CCD. The diagram shows the charge transfer at different stages in time and space.

I. INTRODUCTION

CHARGE TRANSFER INEFFICIENCY (CTI) is an important aspect in the CCD development for operation in High Energy Physics colliders [1]–[3], [18]. The Linear Collider Flavour Identification (LCFI) collaboration has been developing new CCD chips and testing them for about 10 years [1]–[5], [18]. Recently the focus of the simulations has been on CCDs with column parallel readout (CPCCD). Full simulations of a simplified model of this device have been performed with the Integrated Systems Engineering Technology Computer Aided Design (ISE-TCAD) package version 7.5, particularly the DESSIS program (Device Simulation for Smart Integrated System). Full TCAD simulations for a CPCCD were performed for different readout frequencies and operating temperatures [6]–[8]. Full TCAD simulations are very CPU intensive. This has already been noted for the CCD simulations with a sequential readout [9]–[11]. We expect the TCAD simulation to describe well the shape of the CTI. The CTI depends on many parameters, such as readout frequency and operating temperature. Some parameters are related to the trap characteristics like trap energy level, capture cross-section and trap concentration (density). Other factors are also relevant, such as the occupancy of the pixels (hits). It is well known that analytic charge transfer models can be used to study the CTI dependence on readout frequency and operating temperature [12]–[14]. For a comparison with full TCAD CTI simulation results, we have developed Analytic Models for the CPCCD [6]–[8]. The further development of these Analytic Models leads also to better understanding of the relevant parameters in order to reduce the CTI in future CPCCD prototypes. This paper addresses the inclusion of signal shape and clock voltage amplitude which leads to an improved Analytic Model for a CPCCD. The CTI obtained from the improved Analytic Model is compared with results from full TCAD simulations.

II. ANALYTIC MODEL FOR CTI DETERMINATION

The Analytic Models [6]–[8] describe the different steps in the charge transfer process and the amount of the trapped charge with respect to the charge cloud in transfer. Fig. 1 shows the consecutive charge transfer for a two-phase CPCCD in one pixel (2 nodes). Following the treatment by Kim [15], based on earlier work by Shockley, Read and Hall [16], [19] a defect at an energy below the bottom of the conduction band is considered. Our

Manuscript received November 15, 2008; revised March 19, 2009 and April 03, 2009. Current version published June 17, 2009. This work was supported by the Science and Technology Facilities Council (STFC) and Lancaster University. S. Aoulmit, K. Bekhouche, and L. Dehimi thank the Algerian Government for support. A. Sopczak thanks the Faculty of Science and Technology at Lancaster University for support. This work was presented on behalf of the LCFI Collaboration

A. Sopczak, K. Bekhouche, C. Bowdery, and M. Koziel are with Lancaster University, Lancaster LA1 4YW, U.K. (e-mail: andre.sopczak@cern.ch).

S. Aoulmit, D. Djendaoui, and L. Dehimi are with LMSM Laboratory, Biskra University, 07000 Biskra, Algeria.

C. Buttar and D. Maneuski are with Glasgow University, Glasgow G12 8QQ, U.K.

C. Damerell, K. Stefanov, and S. Worm are with STFC Rutherford Appleton Laboratory, Didcot OX11 0QX, U.K.

T. Greenshaw, T. Tikkanen, and T. Woolliscroft are with Liverpool University, Liverpool L69 3BX, U.K.

A. Nomerotski is with Oxford University, Oxford OX1 2JD, U.K.

Color versions of one or more of the figures in this paper are available online at http://ieeexplore.ieee.org.

Digital Object Identifier 10.1109/TNS.2009.2020985

model considers one single energy level and includes the emission time, τ_e, and capture time, τ_c, constants in the differential equation

$$\frac{dr}{dt} = \frac{1-r}{\tau_c} - \frac{r}{\tau_e} \tag{1}$$

where r is the fraction of filled traps. Initially the fraction of filled traps is $r(0)$. At stage A the signal charge packet arrives and interacts with traps under node 1 during time t_1. This interaction leads to the capture and emission process. By solving the differential equation (1), the fraction of filled traps r_{1A} under node 1 during time t_1 (when the signal packet is present) is given by the equation

$$r_{1A}(t_1) = \left[(r(0) - \frac{\tau_s}{\tau_c}\right] \exp\left(-\frac{t_1}{\tau_s}\right) + \frac{\tau_s}{\tau_c} \tag{2}$$

where $\tau_s = \tau_c \tau_e / (\tau_c + \tau_e)$.

At stage B charge moves to the next node and interacts with traps during time t_2 under this node. During time t_2 electrons emitted from node 1 join the signal charge packet in the second node. Thus, the fraction of filled traps r_{1B} under node 1 during time t_2 in the absence of the signal packet is given by the equation

$$r_{1B}(t_2) = r_{1A}(t_1) \exp\left(-\frac{t_2}{\tau_e}\right). \tag{3}$$

At the same stage B, r_{2B} is defined as the fraction of filled traps under node 2 during time t_2. Thus,

$$r_{2B}(t_2) = \left[r(0) - \frac{\tau_s}{\tau_c}\right] \exp\left(-\frac{t_2}{\tau_s}\right) + \frac{\tau_s}{\tau_c}. \tag{4}$$

When the signal charge moves to the first node of the next pixel, stage C, electrons emitted during time t_1 can join the signal present at this node and the fraction of filled traps r_{2C} under node 2 during time t_1 is given by

$$r_{2C}(t_1) = r_{2B}(t_2) \exp\left(-\frac{t_1}{\tau_e}\right). \tag{5}$$

The CTI is defined by the ratio of the charge loss under each node to the signal charge density n_s, thus,

$$\mathrm{CTI} = \frac{N_t}{n_s}[r_{1B}(t_2) + r_{2C}(t_1) - 2r(0)] \tag{6}$$

where N_t is the trap concentration and the background state $r(0) = \exp(-t_w/\tau_e)$ is determined by considering that initially all traps are filled and electrons are emitted during the waiting time t_w which is the time between two signal charge packets. For the case $t_1 = t_2 = t$, the combination of the previous equations leads to

$$\begin{aligned}\mathrm{CTI} = 2\frac{N_t}{n_s}&\left[1 - \exp\left(-t\left(\frac{1}{\tau_c} + \frac{2}{\tau_e}\right)\right)\right] \\ &\times \left[\left(\frac{\tau_s}{\tau_c} \frac{\left(1 - \exp\left(-\frac{t}{\tau_s}\right)\right)}{\left(1 - \exp\left(-t\left(\frac{1}{\tau_s} + \frac{1}{\tau_e}\right)\right)\right)}\right) \exp\left(-\frac{t}{\tau_e}\right)\right. \\ &\left. - \exp\left(-\frac{t_w}{\tau_e}\right)\right]. \end{aligned} \tag{7}$$

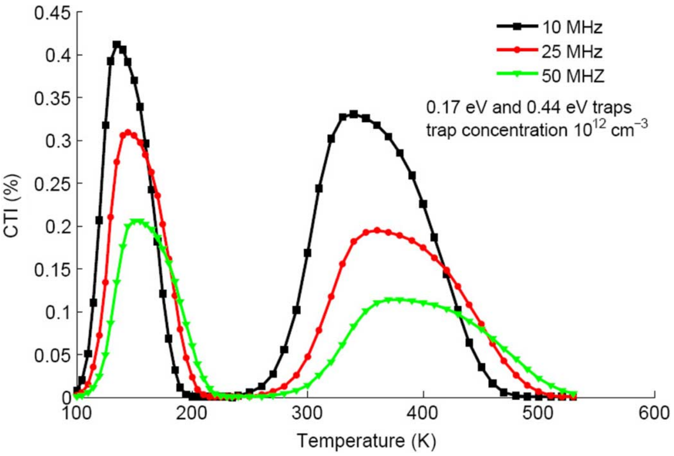

Fig. 2. CTI values from an Analytic Model as a function of temperature in a two-phase CPCCD for the two traps, 0.17 eV and 0.44 eV with a concentration of 10^{12} cm^{-3} and 1% hit (pixel) occupancy at readout frequencies 10, 25 and 50 MHz.

The Analytic Model assumes that the signal charge moves instantaneously from one node to the next and does not consider edge effects in the signal charge transfer.

III. ANALYTIC MODEL CTI RESULTS

The CTI dependence on readout frequency and operating temperature has been explored using an Analytic Model based on (7). Fig. 2 shows the CTI results from the Analytic Model at different frequencies for temperatures between 100 K and 550 K. The CTI increases as the readout frequency decreases. For higher readout frequencies there is less time to trap the charge, thus the CTI is reduced. At high temperatures the emission time is so short that the trapped charges can rejoin the passing signal.

IV. COMPARISON BETWEEN FULL TCAD SIMULATION AND ANALYTIC MODEL REGARDING SIGNAL SHAPE EFFECT

The implementation of a more realistic signal shape into the Analytic Model is expected to improve the agreement with the full TCAD simulation. The signal charge profile varies in the signal cloud as illustrated in the upper part of Fig. 3. The signal packet does not have well defined boundaries and the charge concentration decreases gradually from the center of the signal packet. Therefore, the signal packet will interact with a varying fraction of the traps within the pixel and this affects the CTI determination. Fig. 4 shows the shape of the profile of the signal charge under the node from a full TCAD simulation. The signal charge used in the simulation is chosen to be similar to the charge generated by a minimum ionising particle (MIP). The maximum value taken for the signal charge is 4.5×10^{14} cm^{-3}. Two-dimensional and one-dimensional signal charge density profiles are extracted as shown in Figs. 5 and 6, respectively. The effect of signal charge profile is studied by means of the capture time. We simulated the charge transfer in a CPCCD considering two bulk traps with energies 0.17 eV and 0.44 eV below the conduction band. The 0.17 eV trap is an oxygen-vacancy defect, referred to as an A-center defect. The

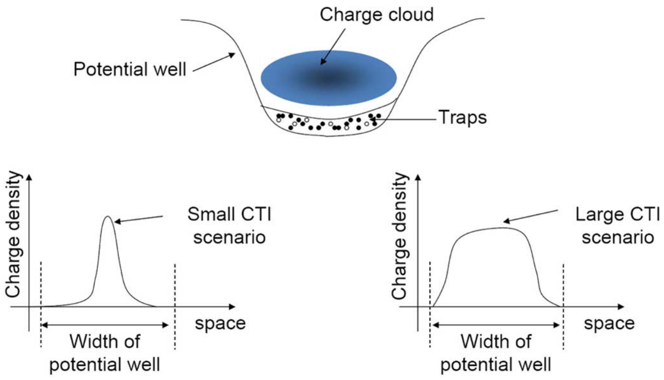

Fig. 3. Diagram of the signal packet in a potential well and effect of the signal shape on the expected CTI. Upper part: the density of a signal packet in a potential well decreases gradually from the center of the packet. Lower part: expected scenario of the CTI dependence on the shape of the signal packet (small CTI for a narrow shape as shown on the left-hand side and large CTI for a wider shape as shown on the right-hand side).

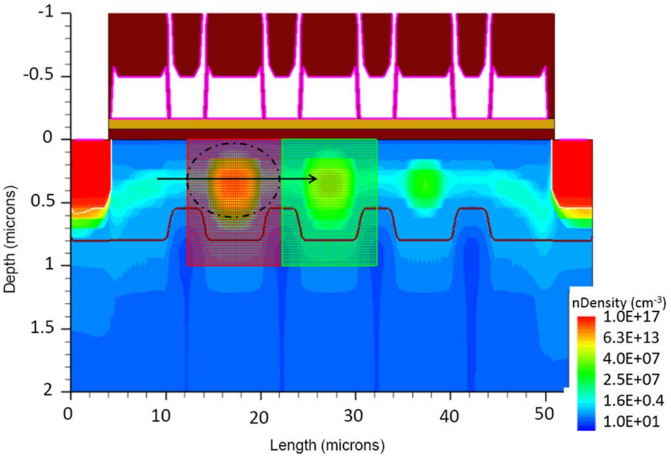

Fig. 4. Signal charge density in transit from a TCAD simulation of a CPCCD. The plot shows the charge packet located under a node at a depth of about 0.5 microns. One pixel is located between $x = 10$ and 30 microns. The arrow indicates the direction of the transfer.

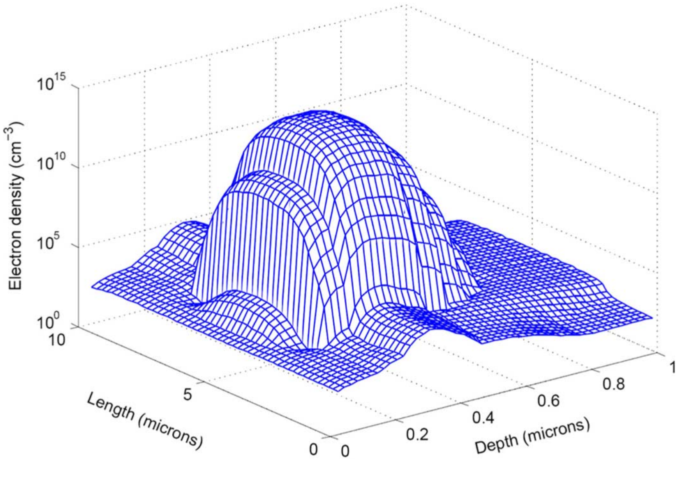

Fig. 5. Two-dimensional signal charge density extracted from the charge packet under one node using a full TCAD simulation.

0.44 eV trap is a phosphorous-vacancy defect, referred to as an E-center [1], [2], [18], [17].

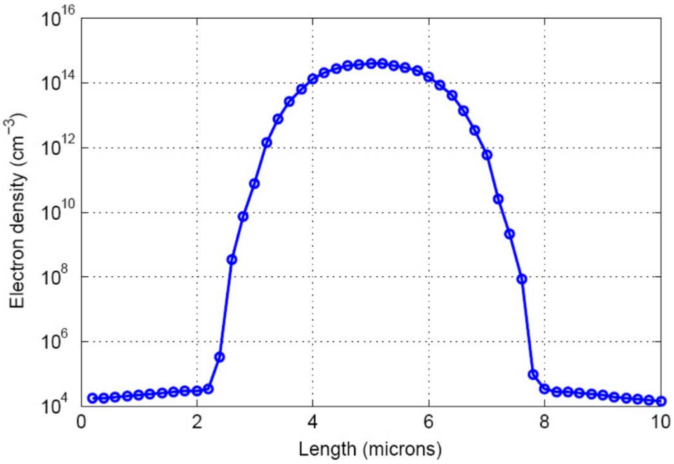

Fig. 6. One-dimensional signal charge density extracted from the charge packet under one node using a full TCAD simulation at a depth of 0.5 microns.

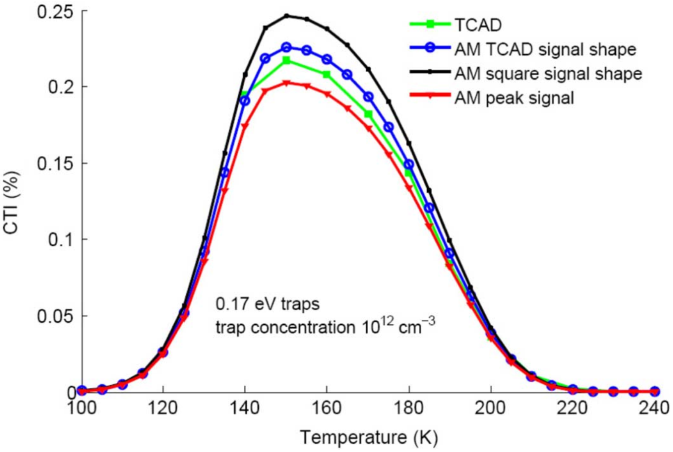

Fig. 7. CTI from Analytic Model (AM) including the shape of the signal packet as a function of temperature for 0.17 eV traps with a concentration of 10^{12} cm^{-3} and 1% hit (pixel) occupancy at 50 MHz readout frequency in comparison with full TCAD simulation results. Three different signal shapes are compared with the full TCAD simulation. The CTI calculation with the Analytic Model using the signal shape extracted from a full TCAD simulation agrees better with the full TCAD simulation results than those from the Analytic Model using a square-shape signal as assumed previously.

Figs. 7 and 8 show the CTI dependence on the signal charge profile for the 0.17 eV and 0.44 eV traps at 50 MHz. These figures also show the CTI values for different signal shapes in comparison with the full TCAD simulation. The CTI is reduced as the width of the potential well becomes smaller. This behavior is expected, as illustrated in the lower part of Fig. 3. The CTI values calculated with the Analytic Model including the signal charge profile agree better with the full TCAD simulation results for the 0.17 eV traps (Fig. 7). The relatively shallow traps (0.17 eV) are more affected by the signal charge shape than the deeper ones (0.44 eV). For the latter, the minor effect of the signal charge profile is due to its small capture cross-section. The inclusion of the approximate signal shape in the Analytic Model reduces the CTI value in the peak region by about 10 to 20% compared to assuming a square-shape signal. For different signal shapes Fig. 9 shows the ratio of the CTI from Analytic Model to CTI from full TCAD simulation for the 0.17 eV traps

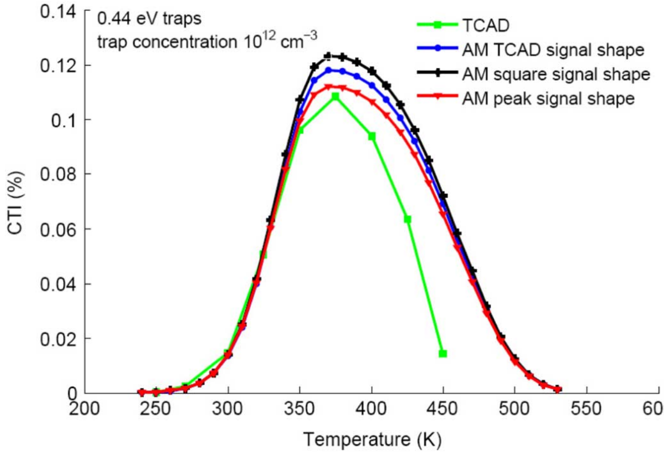

Fig. 8. CTI from Analytic Model (AM) including the shape of the signal packet as a function of temperature for 0.44 eV traps with a concentration of 10^{12} cm^{-3} and 1% hit (pixel) occupancy at 50 MHz readout frequency in comparison with full TCAD simulation results. Three different signal shapes are compared with the full TCAD simulation. For the 0.44 eV traps the inclusion of the signal shape in the Analytic Model has only a small effect to improve the agreement with the full TCAD simulation.

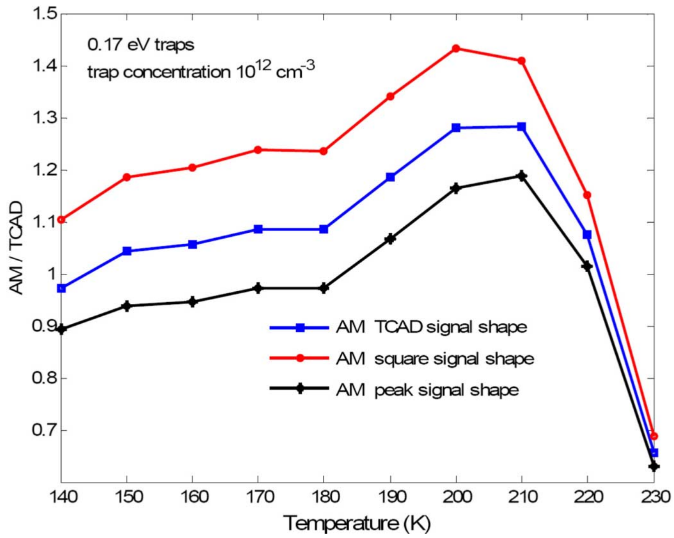

Fig. 9. Ratio of CTI from Analytic Model (AM) with different signal shapes to CTI from full TCAD simulation for 0.17 eV traps at 50 MHz readout frequency.

at 50 MHz readout frequency. We see that the results of the Analytic Model with the TCAD signal shape agree better with the full TCAD simulation than the square and peak shapes. Similar results are obtained for 0.44 eV traps below the temperature 350 K.

V. Comparison Between Full TCAD Simulation and Analytic Model Regarding Clock Voltage Effect

In this study the effect of different clock voltage amplitudes on CTI values are investigated. A sine voltage form is applied to consecutive nodes as shown in Fig. 10. The following variables are defined:

V_1: voltage applied to a first node of a pixel,
V_2: voltage applied to a second node of a pixel,
V_B: potential barrier created between two successive gates by the doping profile,
$T_{1,3}$: time interval where $|V_1 - V_2| < V_B$,
T_2: time interval where $|V_1 - V_2| > V_B$.

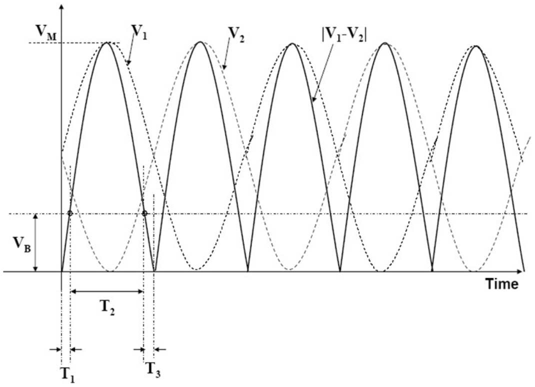

Fig. 10. Diagram of clock voltages in a two-phase CPCCD. V_1 and V_2 (dashed lines) show the applied voltages under node 1 and 2, respectively. The solid line shows the difference between the two applied voltages. V_B is the barrier potential (horizontal dashed line). T_1 and T_3 are time periods with no charge transfer and T_2 is the time period with charge transfer.

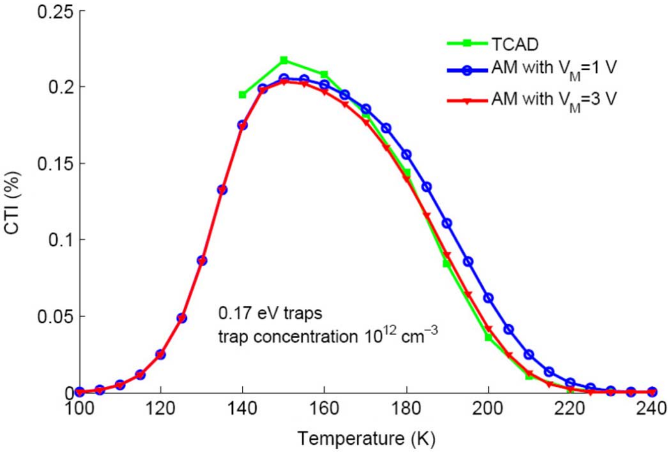

Fig. 11. CTI from Analytic Model (AM) including clock voltage effects as a function of temperature for 0.17 eV traps with a concentration of 10^{12} cm^{-3} and 1% hit (pixel) occupancy at 50 MHz readout frequency in comparison with full TCAD simulation results. Two different clock voltages (V_M) are shown.

The signal is not transferred until the difference between the two clock voltages V_1 and V_2 reaches the potential barrier created between two consecutive nodes. This affects the CTI determination and it is now included in the Analytic Model. The time intervals T_1 and T_3 are defined by the intersection point between the $|V_1 - V_2|$ curve and the barrier potential V_B (horizontal dashed line). Thus,

$$T_1 = T_3 = \frac{1}{2\pi f} \times \sin^{-1}\left(\frac{V_B}{V_M}\right) \tag{8}$$

where V_M is the amplitude of the clock voltage.

The CTI determined with the Analytic Model including the clock voltage effect is shown in Figs. 11 and 12 for 0.17 eV and 0.44 eV traps, respectively. Two different clock voltage amplitudes are used to illustrate the effect of the clock voltage and to compare with full TCAD simulations which use 3 V as induced voltage. It is noted that the CTI decrease occurs only for temperatures above the CTI peak position. At high temperature, the

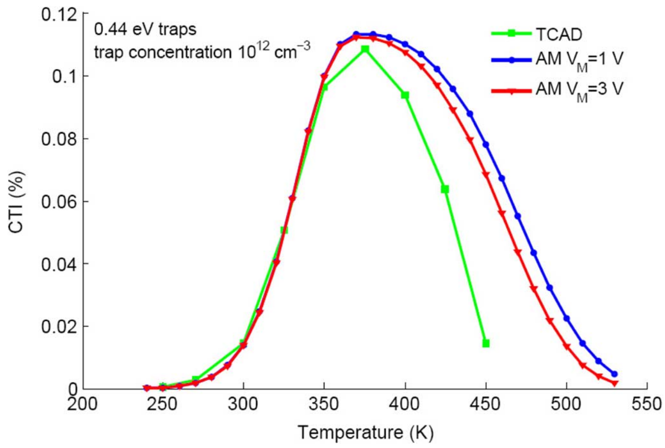

Fig. 12. CTI from Analytic Model (AM) including the clock voltage effects as a function of temperature for 0.44 eV traps with a concentration of 10^{12} cm^{-3} and 1% hit (pixel) occupancy at 50 MHz readout frequency in comparison with full TCAD simulation results. Two different clock voltages (V_M) are shown.

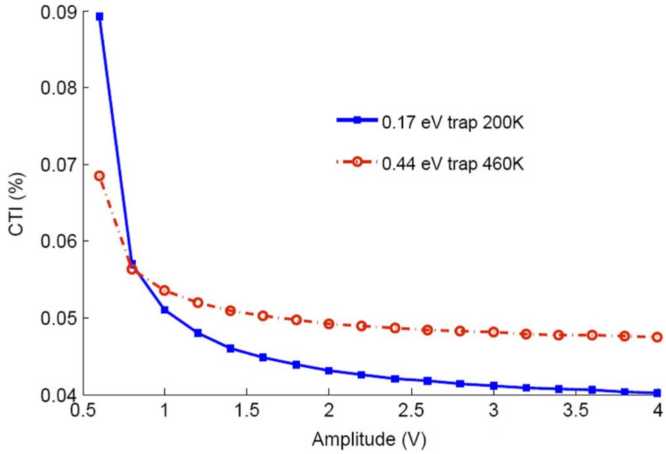

Fig. 13. CTI from Analytic Model as a function of clock voltage amplitude for both traps 0.17 eV and 0.44 eV with a concentration of 10^{12} cm^{-3} at $T = 200$ K and $T = 460$ K, respectively, with 1% hit (pixel) occupancy and 50 MHz readout frequency.

emission time constant decreases to become comparable to the joining time. Now trapped electrons rejoin their signal packet and CTI decreases. When clock voltage increases the joining time increases and there is more time for electrons to rejoin their signal packet.

In addition, the effect of the clock voltage amplitude on the CTI is studied for a large variation of amplitudes. The CTI decreases as the amplitude increases until it saturates and no further decrease can be observed. This result is shown in Fig. 13 for two examples, 0.17 eV traps at a temperature of 200 K and 0.44 eV traps at a temperature of 460 K.

VI. CONCLUSIONS AND OUTLOOK

Our previous Analytic Model for a CPCCD has been extended to include the effect of non-uniform signal shape and the effect of realistic clock voltage amplitudes for CTI calculations. The signal shape affects the CTI mostly in the peak region. A smaller width of the potential well decreases the CTI. The inclusion of the clock voltage effects leads to smaller CTI values only above the CTI peak position (for high temperatures). In summary, the Analytic Model has been extended to give a more realistic description of the CTI for a CPCCD and the results agree better with full TCAD simulations. Overall, the Analytic Model predicts well the CTI peak position in comparison with a full TCAD simulation. It can produce CTI values almost instantly while the full TCAD simulation is very CPU intensive. Generally, agreement between the Analytic Model and full TCAD simulation results is good for the 0.17 eV traps while for the 0.44 eV traps the results of the Analytic Model do not agree with the full TCAD simulation in a range above 375 K which is above normal operating temperature. The Analytic Model is suited to contribute to future CPCCD developments.

ACKNOWLEDGMENT

S. Aoulmit, K. Bekhouche, and L. Dehimi would like to thank Lancaster University for its hospitality. A. Sopczak thanks the organizers of the IEEE'08 conference for their hospitality.

REFERENCES

[1] C. J. S. Damerell, "Radiation damage in CCDs used as particle detectors," *ICFA Instrum. Bull.*, vol. 14, 1997.

[2] K. Stefanov, "Radiation damage effects in CCD sensors for tracking applications in high energy physics," Ph.D. dissertation, Saga Univ., Saga, Japan, 2001.

[3] LCFI Collaboration [Online]. Available: http://hepwww.rl.ac.uk/lcfi

[4] S. D. Worm, "Recent CCD developments for the vertex detector of the ILC—Including ISIS (in-situ storage image sensors)," in *Proc. 10th Topical Seminar Innovative Particle and Radiation Detectors (IPRD06)*, Siena, Italy, Oct. 1–5, 2006.

[5] T. J. Greenshaw, "Column parallel CCDs and in-situ storage image sensors for the vertex detector of the international linear collider," in *Proc. Nuclear Science Symp.*, San Diego, CA, Oct. 29–Nov. 4 2006.

[6] A. Sopczak *et al.*, "Radiation hardness studies in a CCD with high-speed column parallel readout," in *Proc. 10th ICATPP Conf. Astroparticle, Particle, Space Physics, Detectors and Medical Physics Applications*, Como, Italy, Oct. 8-12, 2007, p. 599.

[7] A. Sopczak *et al.*, "Radiation hardness studies in a CCD with high-speed column parallel readout," in *Proc. IEEE Nuclear Science Symp. Conf. Rec.*, Honolulu, HI, 2007, vol. N48-2, p. 2278.

[8] A. Sopczak *et al.*, "Radiation hardness studies in a CCD with high-speed column parallel readout," *J. Inst.*, vol. 3, p. 5007, 2008.

[9] A. Sopczak *et al.*, "Simulation of the temperature dependence of the charge transfer inefficiency in a high-speed CCD," *IEEE Trans. Nucl. Sci.*, vol. 54, no. 4, pp. 1429–1434, Aug. 2007.

[10] A. Sopczak *et al.*, "Radiation hardness of CCD vertex detectors," in *Proc. IEEE Nuclear Science Symp. Conf. Rec.*, San Juan, PR, 2005, vol. N37-7, p. 1494.

[11] A. Sopczak *et al.*, "Radiation hardness CCD vertex detectors for the ILC," in *Proc. IEEE Nuclear Science Symp. Conf. Rec.*, San Diego, CA, 2006, vol. N14-215, p. 576.

[12] A. M. Mohsen and M. F. Tompsett, "The effects of bulk traps on the performance of bulk channel charge-coupled devices," *IEEE Trans. Electron Devices*, vol. ED-21, no. 11, p. 701, 1974.

[13] I. H. Hopkins, G. Hopkinson, and B. Johlander, "Proton-induced charge transfer degradation in CCD's for near-room temperature applications," *IEEE Trans. Nucl. Sci.*, vol. 41, no. 6, pp. 1984–1991, Dec. 1994.

[14] T. Hardy, R. Murowinski, and M. J. Deen, "Charge transfer efficiency in proton damaged CCD's," *IEEE Trans. Nucl. Sci.*, vol. 45, no. 2, pp. 154–163, Apr. 1998.

[15] Ch.-K. Kim, M. J. Howes, and D. V. Morgan*, Charge-Coupled Devices and Systems*. New York: Wiley, 1979, p. 57.

[16] W. Shockley and W. T. Read, "Statistics of the recombinations of holes and electrons," *Phys. Rev.*, vol. 87, p. 835, 1952.

[17] J. Janesick, T. Elliot, and F. Pool, "Radiation damage in scientific charge-coupled devices," *IEEE Trans. Nucl. Sci.*, vol. 36, no. 1, pp. 572–578, Feb. 1989.

[18] K. Stefanov *et al.*, "Electron and neutron radiation damage effects on a two-phase CCD," *IEEE Trans. Nucl. Sci.*, vol. 47, no. 3, pp. 1280–1291, Jun. 2000.

[19] R. N. Hall, "Electron-hole recombination in germanium," *Phys. Rev.*, vol. 87, p. 387, 1952.